# Leaf Area Index identified as a major source of variability in modelled CO₂ fertilization

Qianyu Li[1,5], Xingjie Lu[2], Yingping Wang[3], Xin Huang[4], Peter M. Cox[5], Yiqi Luo[1,2]

[1]Ministry of Education Key Laboratory for Earth System Modeling, Department of Earth System Science, Tsinghua University, Beijing 100084, China

[2] Center for Ecosystem Science and Society (Ecoss), Northern Arizona University, Flagstaff, AZ 86011, USA

[3]CSIRO Marine and Atmospheric Research, Centre for Australian Weather and Climate Research, PMB #1, Aspendale, Victoria 3195, Australia

[4]Department of Computer Science and Technology, Tsinghua University, Beijing 100084, China

[5]College of Engineering, Mathematics and Physical Sciences, University of Exeter, Exeter, EX4 4QF, UK

*Correspondence to*: Yiqi Luo (luoyiqi@mail.tsinghua.edu.cn)

15

**Abstract.** The concentration-carbon feedback factor ($\beta$), also called the $CO_2$ fertilization effect, is a key unknown in climate-

20  carbon cycle projections. A better understanding of model mechanisms that govern terrestrial ecosystem responses to elevated

$CO_2$ is urgently needed to enable a more accurate prediction of future terrestrial carbon sink. We calculated $CO_2$ fertilization

effects at various hierarchical levels from leaf biochemical reaction, leaf photosynthesis, canopy gross primary production

(GPP), net primary production (NPP), to ecosystem carbon storage (*cpool*), for seven $C_3$ vegetation types in response to

increasing $CO_2$ under RCP 8.5 scenario, using the Community Atmosphere Biosphere Land Exchange model (CABLE). Our

25  results show that coefficient of variation (CV) for the CABLE model among the seven vegetation types is 0.15-0.13 for the

biochemical level $\beta$, 0.13-0.16 for the leaf-level $\beta$, 0.48 for the $\beta_{GPP}$, 0.45 for the $\beta_{NPP}$, and 0.58 for the $\beta_{cpool}$. The low

variation of the leaf-level $\beta$ is consistent with a theoretical analysis that leaf photosynthetic sensitivity to increasing $CO_2$

concentration is almost an invariant function. In CABLE, the major jump in CV of $\beta$ values from leaf- to canopy- and

ecosystem-levels results from divergence in modelled leaf area index (LAI) within and among the vegetation types. The

30  correlations of $\beta_{GPP}$, $\beta_{NPP}$, or $\beta_{cpool}$ with $\beta_{LAI}$ are very high in CABLE. Overall, our results indicate that modelled LAI is

a key factor causing the divergence in $\beta$ values in CABLE model. It is therefore urgent to constrain processes that regulate

LAI dynamics in order to better represent the response of ecosystem productivity to increasing $CO_2$ in Earth System Models.

35

40

## 1. Introduction

Terrestrial carbon sink, taking up roughly 30% of anthropogenic $CO_2$ emissions, is of great uncertainty and vulnerable to global climate change (Le Quéré et al., 2015; Cox et al., 2000). The $CO_2$ fertilizing effect, also called the concentration-carbon feedback factor ($\beta$), has been identified as a major uncertainty in modeling terrestrial ecosystem response to future climate

45    change. In Coupled Model Intercomparison Project (C4MIP) and Coupled Model Intercomparison Project Phase 5 (CMIP5), all models agree that terrestrial carbon sink will gradually saturate in the future but disagree on the magnitude of $\beta$ (Friedlingstein et al., 2006; Arora et al., 2013; Friedlingstein et al., 2015). Some studies pointed out that the contribution of $\beta$ is 4 or 4.5 times larger, and more uncertain, than carbon-climate feedback factor ($\gamma$) (Gregory et al., 2009; Bonan & Levis, 2010; Arora et al., 2013). Apart from the substantial uncertainty among different models, Smith et al. (2016) suggested that

50    Earth System Models (ESMs) in CMIP5 overestimate global terrestrial $\beta$ values compared with remote sensing data and Free-Air $CO_2$ Enrichment (FACE) experiment results. The large disparity between models and reality gives us little confidence in making policies to combat global warming.

Efforts have been made to identify causes for the diverse ecosystem responses to $eCO_2$ and increasing temperature in models.

55    For example, Zeng (2004) used different parameterizations of $CO_2$ fertilization, soil decomposition rate and turnover time to explain the total land carbon change in a coupled earth system model. Matthews et al. (2005) showed different parameterizations of temperature constraints on photosynthesis strongly affects $\gamma$ results. Tachiiri et al. (2012) found the maximum photosynthesis rate ($V_{cmax}$) and specific leaf area (SLA, leaf area per unit dry mass) had the most significant contributions to both of $\beta$ and $\gamma$ with a ESMs emulator. To gain insight into the characteristics of biogeochemical cycles $\beta$

60    and $\gamma$, it's necessary to identify sensitive parameters and important processes in models from a mechanistic way.

The response of ecosystem carbon cycle to $eCO_2$ is primarily driven by stimulation of leaf-level carboxylation rate in plants by $eCO_2$ (Long et al., 2004; Heimann et al., 2008). The $CO_2$ stimulation of carboxylation then translates into increasing GPP and NPP, possibly leading to increased biomass and soil carbon storage and slowing down anthropogenically driven increase

65    in atmospheric $CO_2$ (Canadell et al., 2007; Iversen et al., 2012; De Kauwe et al., 2014). The leaf-level $CO_2$ fertilization is

generally well characterized with models from Farquhar et al. (1980) and Collatz et al. (1991, 1992), which have been adopted

by most land surface models (Bonan et al., 2013; Wang et al., 1998; Cox, 2001). Previous research with both theoretical

analysis and data synthesis from a large number of experiments has revealed that normalized $CO_2$ sensitivity of leaf-level

photosynthesis, which represents kinetics sensitivity of photosynthetic enzymes, varies little among different vegetation types

70    at a given $CO_2$ concentration (Luo & Monney, 1996; Luo et al., 1996). However, the $CO_2$ fertilization effects are considerably

more variable at canopy- and ecosystem-level than at the leaf-level, because a cascade of uncertain processes, such as soil

moisture and canopy structure, influence GPP, NPP and carbon storage (Friedlingstein et al., 2015; Fatichi et al., 2016).

Amongst these processes, leaf area index (LAI) largely affects canopy assimilation and plant growth under condition of $eCO_2$,

and representation of LAI in plant productivity models causes large uncertainty (Ewert, 2004). Models generally predict that

75    LAI dynamics will respond to $eCO_2$ positively due to enhanced leaf biomass, then increasing LAI will in turn feed back to

greater canopy GPP as a result of more light interception. However, the relative contributions of the response of leaf-level

photosynthesis and LAI to $\beta$ of GPP have been rarely quantified and compared in previous studies. Therefore, understanding

which processes in ecosystem models amplify variability in $\beta$ from biochemical and leaf levels to canopy and ecosystem

levels is quite important.

80

As to the spatial pattern, the largest absolute $CO_2$ fertilizing effects at ecosystem level were found in tropical regions mainly

because of high basic NPP (Joos et al., 2001; Peng et al., 2014). But the variation of relative $\beta$ effects across different

geographical locations and vegetation types and the dominating factors are rarely discussed and often ignored. In this study,

we tried to answer the following questions: how and why $\beta$ values at different hierarchical levels vary across different

85    geographical locations and vegetation types? We used Community Atmosphere Biosphere Land Exchange model (CABLE)

to identify key mechanisms driving diverse $\beta$ values under RCP 8.5 scenario within and across seven $C_3$ vegetation types.

## 2. Materials and methods

### 2.1 CABLE model description

CABLE (version 2.0) is a global land surface model as described by Wang et al. (2010, 2011) and is improved by including

90    global carbon, nitrogen and phosphorus cycles. To simplify the study, phosphorus and nitrogen cycles are not used. Leaf

photosynthesis, stomatal conductance, and heat and water transfer in CABLE are calculated using the two-leaf approach (Wang

& Leuning, 1998) for both sunlit leaves and shaded leaves. The distinction between sunlit and shaded leaves is necessary in

scaling from leaf to canopy because the response of photosynthesis to the absorbed photosynthetically active radiation (PAR)

is nonlinear. The two-leaf model uses the same set of equations for calculating photosynthesis, transpiration and sensible heat

95    fluxes for an individual leaf, but with the bulk formulation for the parameters for all sunlit and shaded leaves separately. For a

given leaf parameter $P$, the corresponding parameter values for the two big leaves are calculated as:

$$P_1 = \int_0^\Lambda p(\lambda) f_{sun}(\lambda) d\lambda \quad \text{(big sunlit leaves)} \tag{1}$$

$$P_2 = \int_0^\Lambda p(\lambda) \left(1 - f_{sun}(\lambda)\right) d\lambda \quad \text{(big shaded leaves)} \tag{2}$$

$f_{sun}$ is the fraction of sunlit leaves within a canopy, calculated by $f_{sun} = \exp(-k_b \lambda)$, where $k_b$ is the extinction coefficient of

100    direct beam radiation for a canopy with black leaves. $\lambda$ is cumulative LAI.

CABLE calculates plant photosynthesis rate according to Leuning (1990). Leuning (1990) described a method to calculate

stomatal conductance, $CO_2$ assimilation, and intercellular $CO_2$, by solving equations describing the supply of $CO_2$ through

stomata and demand for $CO_2$ in photosynthesis (Farquhar et al., 1980) simultaneously. Since $C_3$ plants have similar

105    mechanisms for photosynthesis and respond to $eCO_2$ much stronger than $C_4$ plants, $C_3$ plants are only considered in this study.

Canopy net photosynthesis rate is calculated as:

$$A = \min\{A_c, A_q, A_p\} - R_d = G_{st}(C_S - C_i) \tag{3}$$

$$A_c = V_{cmaxbig} * \frac{C_i - \Gamma_*}{C_i + K_c(1 + O_i - K_O)} \tag{4}$$

$$A_q = J_{cmaxbig} * \frac{C_i - \Gamma_*}{C_i + 2\Gamma_*} \tag{5}$$

110 $$A_p = 0.5 * V_{cmaxbig} \tag{6}$$

Where $A_c, A_q$ and $A_p$ are assimilation rates limited by Rubisco activity, RuBP regeneration and sink respectively. $R_d$ is

day respiration, which is proportional to $V_{cmaxbig}$. $V_{cmaxbig}$ is the maximum catalytic activity of Rubisco of big leaves. $C_i$

is intercellular $CO_2$ concentration. $\Gamma_*$ is the $CO_2$ compensation point in the absence of day respiration. $K_c$ and $K_O$ are

Michaelis-Menten constants for $CO_2$ and $O_2$ respectively. $O_i$ is intercellular oxygen concentration. $\Gamma_*$, $K_c$ and $K_O$ are only

115 functions of leaf temperature. $J_{cmaxbig}$ is the maximum rate of photosynthesis at saturating $C_i$ for a given absorbed photo

irradiance of big leaves. For sunlit and shaded leaves, $V_{cmaxbig}$ and $J_{cmaxbig}$ are defined as follows:

$$V_{cmaxbig,1} = v_{cmax,25} * f_{vcmax}(T_{f,1}) * \int_0^\Lambda \exp(-k_b\lambda)\exp(-k_n\lambda)\,d\lambda = v_{cmax,25} * f_{vcmax}(T_{f,1}) * \frac{1-\exp[-LAI(k_n+k_b)]}{k_n+k_b} \tag{7}$$

$$V_{cmaxbig,2} = v_{cmax,25} * f_{vcmax}(T_{f,2}) * \int_0^\Lambda [1 - \exp(-k_b\lambda)]\exp(-k_n\lambda)\,d\lambda = v_{cmax,25} * f_{vcmax}(T_{f,2}) * \left\{ \frac{1-\exp(-k_n LAI)}{k_n} - \right.$$
$$\left. \frac{1-\exp[-LAI(k_n+k_b)]}{k_n+k_b} \right\} \tag{8}$$

120 $$J_{cmaxbig,1} = j_{cmax,25} * f_{jcmax}(T_{f,1}) * \int_0^\Lambda \exp(-k_b\lambda)\exp(-k_n\lambda)\,d\lambda = j_{cmax,25} * f_{jcmax}(T_{f,1}) * \frac{1-\exp[-LAI(k_n+k_b)]}{k_n+k_b} \tag{9}$$

$$J_{cmaxbig,2} = j_{cmax,25} * f_{jcmax}(T_{f,2}) * \int_0^\Lambda [1 - \exp(-k_b\lambda)]\exp(-k_n\lambda)\,d\lambda = j_{cmax,25} * f_{jcmax}(T_{f,2}) * \left\{ \frac{1-\exp(-k_n LAI)}{k_n} - \right.$$
$$\left. \frac{1-\exp[-LAI(k_n+k_b)]}{k_n+k_b} \right\} \tag{10}$$

Where $v_{cmax,25}$ is maximum carboxylation rate when photosynthesis is limited by Rubisco activity of a leaf. $j_{cmax,25}$ is

maximum potential electron transport rate of a leaf. It's assumed $j_{cmax,25} = 2v_{cmax,25}$ in the model. $f_{vcmax}(T_{f,1})$ and

125 $f_{jcmax}(T_{f,1})$ describe the temperature dependence of $v_{cmax,25}$ and $j_{cmax,25}$ for sunlit leaves respectively. $f_{vcmax}(T_{f,2})$ and

$f_{jcmax}(T_{f,2})$ describe the temperature dependence of $v_{cmax,25}$ and $j_{cmax,25}$ for shaded leaves respectively. $k_b$ is extinction

coefficient of a canopy of black leaves for direct beam radiation. $k_n$ is an empirical parameter used to describe the vertical

distribution of leaf nitrogen in the canopy.

$G_{st}$ is stomatal conductance, and is calculated as:

130 
$$G_{st} = G_0 + \frac{a * f_w * A}{(C_s - \Gamma)(1 + D_s / D_0)} \tag{11}$$

Where $G_0$ is stomatal conductance when $A$=0. $a$ and $D_0$ are empirical constants, $f_w$ is an empirical parameter describing

the availability of soil water for plants. A is net assimilation rate in Equ. (3). $C_s$ is $CO_2$ mol fraction at the leaf surface. $\Gamma$ is

$CO_2$ compensation point of photosynthesis. $D_s$ is vapour pressure deficit at the leaf surface.

135    Leaf Area Index (LAI) is calculated as:

$$LAI = C_{leaf} * SLA \tag{12}$$

Where $C_{leaf}$ is leaf carbon pool, SLA is specific leaf area.

In CABLE model, leaf growth is divided into four phases. Phase 1 is from leaf budburst to the beginning of steady leaf growth,

phase 2 is from the start of steady leaf growth to the start of leaf senescence, phase 3 is the period of leaf senescence, and phase

140    4 is from the end of leaf senescence to the start of leaf bud burst. During phase 1, allocation of available carbon to leaf is fixed

to 0.8, and allocation to wood and root are set to 0.1 for woody biomes, and 0 and 0.2 respectively for non-woody biomes.

During steady leaf growth (phase 2), the allocation coefficients are constants but vary from biome to biome, taking their values

from Fung et al. (2005). During phases 3 and 4, the leaf allocation is zero and its phase 2 allocation is divided between wood

and root in proportional to their allocation coefficients. For evergreen biomes, leaf phenology remains at phase 2 throughout

145    the year (Wang et al., 2010). SLA is PFT-specific and does not change through time in this study.

Gross primary production (GPP) is the sum of canopy net photosynthesis rate ($A$) and day respiration ($R_d$). Net primary

production (NPP) is calculated as the difference between GPP and autotrophic respiration (both maintenance and growth

respiration), and acts an input to the compartmental nine-pool carbon cycle model. The network for carbon transfer in the

150    compartmental model is based on CASA' model (Fung et al., 2005), including three vegetation pools (leaf, wood and root),

three litter pools (metabolic litter, structure litter and coarse wood debris), three soil pools (fast soil pool, slow soil pool and

Biogeosciences

Discussions

EGU

Open Access

passive soil pools). Heterotrophic soil respiration is calculated as the sum of the respired $CO_2$ from the decomposition of all litter and soil organic carbon pools (Wang et al., 2010).

## 2.2 Experimental design

155 CABLE was first spun up by using meteorological forcing from Community Climate System Model (CCSM) simulations during 1901 to 1910 repetitively until a steady state was achieved. Hourly meteorological driving data include: temperature, specific humidity, air pressure, downward solar radiation, downward long-wave radiation, rainfall, snowfall, and wind. In order to separate the $CO_2$ fertilization effect from the effect of climate change, climate forcing was held as the average from 1901 to 2100. Atmospheric $CO_2$ concentrations were from the historical period (1901-2010) and from RCP8.5 scenario for

160 2011 to 2100. The spatial resolution of CABLE used here is 1.9°×2.5°.

## 2.3 Calculation of $\beta$ values at five hierarchical levels

We aimed to analyze $CO_2$ fertilization effects from biochemical level ($\mathcal{L}$), leaf photosynthesis ($p$), canopy gross primary production (GPP), net primary production (NPP), and ecosystem carbon storage (*cpool*). $\beta$ values of the five levels were calculated as the normalized sensitivity of those variables to e$CO_2$.

165 Equ. (4) and (5) can be simplified as:

$$A_c = v_{cmax,25} * f_{vcmax}(T_f) * \frac{C_i - \Gamma_*}{C_i + K_c(1 + C_o - K_O)} * S = a_c * S \tag{13}$$

$$A_q = j_{cmax,25} * f_{jcmax}(T_f) * \frac{C_i - \Gamma_*}{C_i + 2\Gamma_*} * S = a_q * S \tag{14}$$

Where $a_c$ and $a_q$ represent leaf-level Rubisco- and RuBP-limit photosynthesis rates respectively:

$$a_c = v_{cmax,25} * f_{vcmax}(T_f) * \frac{C_i - \Gamma_*}{C_i + K_c(1 + C_o - K_O)} \tag{15}$$

170 $$a_q = j_{cmax,25} * f_{jcmax}(T_f) * \frac{C_i - \Gamma_*}{C_i + 2\Gamma_*} \tag{16}$$

$S$ indicates the scaling factor that scales fluxes at the single top leaf of the canopy to whole canopy fluxes. For sunlit leaves:

$$S_{sun} = \frac{1 - \exp[-LAI(k_n + k_b)]}{k_n + k_b} \tag{17}$$

For shaded leaves:

$$S_{sha} = \frac{1 - \exp(-k_n LAI)}{k_n} - \frac{1 - \exp[-LAI(k_n + k_b)]}{k_n + k_b} \tag{18}$$

175     where subscripts "*sun*" and "*sha*" denote the sunlit and shaded components of leaf-level scaling factors.

The rate of photosynthesis is typically RuBP-regeneration-limited when $CO_2$ concentration exceeds 300 ppm (Soolanayakanahally et al., 2009). Our results also show that photosynthesis rate under RCP8.5 scenario is mainly RuBP-regeneration-limited (results not shown). Leaf-level $\beta_p$ for sunlit leaf and shaded leaf are defined as:

180    
$$\beta_{p_{sun}} = \frac{1}{p_{sun}} * \frac{dp_{sun}}{dC_a} = \frac{1}{a_{qsun}} * \frac{da_{qsun}}{dC_{isun}} * \frac{dC_{isun}}{dC_a} = \mathcal{L}_{sun} * \frac{dC_{isun}}{dC_a} \tag{19}$$

$$\beta_{p_{sha}} = \frac{1}{p_{sha}} * \frac{dp_{sha}}{dC_a} = \frac{1}{a_{qsha}} * \frac{da_{qsha}}{dC_{isha}} * \frac{dC_{isha}}{dC_a} = \mathcal{L}_{sha} * \frac{dC_{isha}}{dC_a} \tag{20}$$

Where $p_{sun}$ and $p_{sha}$ are leaf-level photosynthesis rates for sunlit leaf and shaded leaf respectively. $C_a$ is atmospheric $CO_2$ concentration. $\mathcal{L}$ was first proposed by Luo et al. (1996). $\mathcal{L}$ function is the normalized response of leaf photosynthesis to a small change in $C_i$ and has been suggested to be an invariant function for $C_3$ plants grown in diverse environments. In this

185     study, $\mathcal{L}$ can be used to indicate leaf biochemical response to $eCO_2$. For sunlit leaf and shaded leaf, $\mathcal{L}$ is defined as:

$$\mathcal{L}_{sun} = \frac{1}{a_{qsun}} * \frac{da_{qsun}}{dC_{isun}} = \frac{3 * \Gamma_{*sun}}{(C_{isun} + 2 * \Gamma_{*sun})(C_{isun} - \Gamma_{*sun})} \tag{21}$$

$$\mathcal{L}_{sha} = \frac{1}{a_{qsha}} * \frac{da_{qsha}}{dC_{isha}} = \frac{3 * \Gamma_{*sha}}{(C_{isha} + 2 * \Gamma_{*sha})(C_{isha} - \Gamma_{*sha})} \tag{22}$$

In this study, $\Gamma_{*sun}$ and $\Gamma_{*sha}$ are yearly average $CO_2$ compensation points in the absence of day respiration for sunlit leaf and shaded leaf respectively. Intercellular $CO_2$ concentration ($C_i$) varies significantly at daily, intra-annual and inter-annual

190     basis. We're interested in how $C_i$ responds to $eCO_2$ on an inter-annual basis. So we first outputted hourly $C_i$ then calculated yearly GPP-weighted average $C_i$ for sunlit leaf ($C_{isun}$) and shaded leaf ($C_{isha}$).

Canopy-level $\beta_{GPP}$ is defined as:

$$\beta_{GPP} = \frac{1}{GPP} * \frac{dGPP}{dC_a} \tag{23}$$

195     Where GPP is the average annual GPP between the two adjacent years. dGPP and $dC_a$ are the differences of GPP and $C_a$ between two adjacent years respectively.

The sensitivity of yearly average LAI to $CO_2$ is defined as:

$$\beta_{LAI} = \frac{1}{LAI} * \frac{dLAI}{dC_a} \tag{24}$$

200     Where LAI and dLAI are similarly defined as those about GPP.

Canopy GPP is the sum of sunlit leaf GPP ($GPP_{sun}$) and shaded leaf GPP ($GPP_{sha}$). Big-leaf $\beta_{GPP_{sun}}$ (or $\beta_{GPP_{sha}}$) can be decomposed as the sum of normalized sensitivity of leaf-level $p$: $\beta_{p_{sun}}$ (or $\beta_{p_{sha}}$) and leaf-to-canopy scaling factor: $\beta_{S_{sun}}$ (or $\beta_{S_{sha}}$) as shown in Equ. (23) and Equ. (24). Subscripts "*sun*" and "*sha*" denote the sunlit and shaded components of leaf-level photosynthesis and leaf-to-canopy scaling factors.

205

$$\beta_{GPP_{sun}} = \frac{1}{GPP_{sun}} * \frac{dGPP_{sun}}{dC_a} = \frac{1}{p_{sun}*S_{sun}} * \frac{d(p_{sun}*S_{sun})}{dC_a} = \frac{1}{p_{sun}} * \frac{dp_{sun}}{dC_a} + \frac{1}{S_{sun}} * \frac{dS_{sun}}{dC_a} = \mathcal{L}_{sun} * \frac{dC_{isun}}{dC_a} + \frac{1}{S_{sun}} * \frac{dS_{sun}}{dC_a} = \beta_{p_{sun}} + \beta_{S_{sun}}$$

(25)

$$\beta_{GPP_{sha}} = \frac{1}{GPP_{sha}} * \frac{dGPP_{sha}}{dC_a} = \frac{1}{p_{sha}*S_{sha}} * \frac{d(p_{sha}*S_{sha})}{dC_a} = \frac{1}{p_{sha}} * \frac{dp_{sha}}{dC_a} + \frac{1}{S_{sha}} * \frac{dS_{sha}}{dC_a} = \mathcal{L}_{sha} * \frac{dC_{isha}}{dC_a} + \frac{1}{S_{sha}} * \frac{dS_{sha}}{dC_a} = \beta_{p_{sha}} + \beta_{S_{sha}}$$

(26)

210    Net ecosystem productivity level $\beta_{NPP}$ is defined as:

$$\beta_{NPP} = \frac{1}{NPP} * \frac{dNPP}{dC_a}$$

(27)

Where NPP and dNPP are similarly defined as those about GPP.

Ecosystem carbon storage level $\beta_{cpool}$ is defined as:

215    $$\beta_{cpool} = \frac{1}{cpool} * \frac{dcpool}{dC_a}$$

(28)

Where *cpool* is the average of total ecosystem carbon storage between two adjacent year, d*cpool* is the difference of total ecosystem carbon storage between two adjacent year. Then these normalized sensitivities are of identical units (ppm$^{-1}$) and can be compared with each other.

220    There are ten patches in each model grid in CABLE. Each patch consists of a certain land use type with a specific fraction. We calculated $\beta$ values and their coefficients of variation (CV) across different geographical locations within a specific PFT at different levels to explore the variability of $\beta$ within PFTs. To study the inter-PFTs variation, we grouped parameters such as $\Gamma_{*sun}$, $C_{isun}$ based on PFTs by calculating the mean values. Then we calculated $\beta$ values for each C$_3$ plant and coefficients of variation of $\beta$ values across plant types at different levels.

225    ## 3. Results

### 3.1 Temporal trends of $\beta$ for different vegetation types

At global scale, $\beta_{cpool}$ values for different $C_3$ plants all decline with time from 2011 to 2100 under RCP8.5 scenario (Fig.1).
However, the magnitudes of $\beta_{cpool}$ differ across them, with the highest values occur in deciduous broadleaf forest from
2011 to 2075 and in shrub after 2075, and lowest values in deciduous needleleaf forest and tundra. $\beta_{cpool}$ values for
230    deciduous needleleaf forest and tundra nearly overlap over time.

### 3.2 Variations of intercellular $CO_2$ concentration and $CO_2$ compensation point

The ratios of $C_i$ to $C_a$ ($C_i/C_a$) are approximately constants with $eCO_2$ (Fig.2a and Fig.2b) for each vegetation type. For sunlit
leaf, $C_i/C_a$ values of different vegetation types range from 0.64 to 0.72 with CV=0.03 (Fig.2a). For shaded leaf, the range is
0.70 to 0.76 with CV=0.03 (Fig.2b). Evergreen broadleaf forest has the greatest $C_i/C_a$ value, while deciduous needleleaf
235    forest has the lowest $C_i/C_a$ value. Values of $CO_2$ compensation point in the absence of day respiration ($\Gamma_*$) for a specific
vegetation type do not change through time since we fixed air temperature in model simulation (Fig.2c and Fig.2d). But there
is a huge variance among different $C_3$ plants becauses of different leaf temperature which $\Gamma_*$ values depend on.

### 3.3 Comparison of $\beta$ effects at different hierarchical levels

Coefficient of variation (CV) for biochemical response $\mathcal{L}$, the ratio of the change of intercellular $CO_2$ concentration to the
240    change of ambient $CO_2$ ($dC_i/dC_a$), leaf-level $\beta_p$, $\beta_{LAI}$, $\beta_{GPP}$, $\beta_{NPP}$ and $\beta_{cpool}$ across different geographical locations
within each vegetation type are listed in Table 1. Variations of biochemical and leaf-level responses are relatively smaller than
those at canopy and ecosystem levels within all $C_3$ plants. Divergence of $dC_i/dC_a$ is the smallest. CVs of $\beta_{LAI}$ are the largest
for all the vegetation types. $\beta_{GPP}$ values also greatly differentiate across different geographical locations. CVs of $\beta_{NPP}$ are
very similar to those of $\beta_{GPP}$ for all the vegetation types except for the evergreen needleleaf forest. CVs of $\beta_{cpool}$ are reduced
245    compared with those of $\beta_{NPP}$ for most vegetation types, except for evergreen broadleaf forest and tundra.

With yearly PFT-averaged $C_i$ and $\Gamma_*$ values (Fig.2), $\mathcal{L}_{sun}$, $\mathcal{L}_{sha}$, $\beta_{p_{sun}}$ and $\beta_{p_{sha}}$ were calculated for different vegetation
types, and were plotted together with $\beta_{GPP}$, $\beta_{NPP}$ and $\beta_{cpool}$ at the year 2056 (the middle year within the prediction period)
under RCP8.5 scenario (Fig.3). CV is marked above data points for each variable to indicate degree of variation among $C_3$
250    plants. Results show that at leaf biochemical level, $\mathcal{L}$ factors for sunlit leaf and shaded leaf range from 0.00030 ppm$^{-1}$ to
0.00053 ppm$^{-1}$. Variations of $\mathcal{L}_{sun}$ and $\mathcal{L}_{sha}$ among vegetation types are small (CV=0.15 and 0.13). At leaf photosynthesis
level, the range of values of $\beta_{p_{sun}}$ and $\beta_{p_{sha}}$ for the seven vegetation types is 0.00022 ppm$^{-1}$ to 0.00035 ppm$^{-1}$, and the
variation among vegetation types is not significant (CV=0.13 and 0.16). But $\beta$ values are diverging when scaled up to GPP

level with CV jumping to 0.48 among vegetation types. $\beta$ values of deciduous broadleaf forest and shrub greatly increase

255    from leaf level to GPP level. However, scaling effects do not significantly amplify $\beta_{GPP}$ for deciduous needleleaf forest, tundra and evergreen broadleaf forest. Values and variance of $\beta_{NPP}$ are similar to those of $\beta_{GPP}$ because NPP values linearly correlate with GPP values for all $C_3$ vegetation types (Fig.S4). Magnitudes of $\beta_{cpool}$ for all vegetation types decrease compared with those of $\beta_{NPP}$ and $\beta_{GPP}$. Shrub has the highest $\beta_{GPP}$ and $\beta_{NPP}$ values (around 0.0013 ppm$^{-1}$), but a smaller $\beta_{cpool}$ value compared with deciduous broadleaf forest. Deciduous needleleaf forest has the lowest $\beta_{GPP}$, $\beta_{NPP}$ and

260    $\beta_{cpool}$ values. CV of $\beta_{cpool}$ among vegetation types reaches the highest value (0.58) among all.

To further explore why $\beta$ at canopy and ecosystem levels are diverging across different geographical locations within the same vegetation types, the correlations between $\beta_{GPP}$ and $\beta_{LAI}$ (Fig. S1), $\beta_{NPP}$ and $\beta_{LAI}$ (Fig. S2), $\beta_{cpool}$ and $\beta_{LAI}$ (Fig. S3) were plotted at the year 2056. Results show that $\beta_{GPP}$, $\beta_{NPP}$ and $\beta_{cpool}$ all have significant linear correlations with $\beta_{LAI}$

265    for patches within the same vegetation type, except within evergreen broadleaf forest where the canopy of many patches closes. The correlations between $\beta_{cpool}$ and $\beta_{LAI}$ are weaker than those between $\beta_{NPP}$ and $\beta_{LAI}$. Across different $C_3$ plant types, results also show that $\beta_{LAI}$ linearly correlates with $\beta_{GPP}$, $\beta_{NPP}$ and $\beta_{cpool}$ (Fig. 4a, Fig. 4b and Fig. 4c), but with slopes that gradually decrease from 0.93 to 0.87 and 0.81.

### 3.4 $\beta$ of sunlit and shaded leaves

270    To understand influences of LAI on canopy GPP, we investigate sunlit and shaded leaf GPP. Temporal trends of sunlit leaf GPP (GPP$_{sun}$) and shaded leaf GPP (GPP$_{sha}$) were plotted for each type of $C_3$ plants from 1901 to 2100 in Fig.5. From the beginning of simulation, GPP$_{sha}$ is higher than GPP$_{sun}$ for almost all $C_3$ types. With significant increases of $CO_2$ concentration from 2011, GPP$_{sha}$ responds more drastically than GPP$_{sun}$. Shaded leaf GPP of deciduous broadleaf forest and shrub responds to eCO2 more significantly than other vegetation types. However, a single sunlit leaf has higher photosynthesis

275    rate than a shaded leaf because of more radiation absorbed. Thus, the scaling factor of shaded leaves contributes more to the magnitude and sensitivity of canopy GPP.

Temporal trends were plotted for $\beta_{GPP_{sun}}(\beta_{GPP_{sha}})$ and decomposing factors $\beta_{p_{sun}}$ ($\beta_{p_{sha}}$) and $\beta_{S_{sun}}$ ($\beta_{S_{sha}}$) for each vegetation type (Fig.6). The sensitivities of GPP$_{sun}$ and GPP$_{sha}$ tend to approach zero through time because the decomposing

280    factors $\beta_{p_{sun}}$, $\beta_{p_{sha}}$, $\beta_{S_{sun}}$ and $\beta_{S_{sha}}$ all decline with time.Values of $\beta_{p_{sun}}$ and $\beta_{p_{sha}}$ overlap through time for each vegetation type. Values of $\beta_{GPP_{sha}}$ are higher than those of $\beta_{GPP_{sun}}$ for all $C_3$ vegetation types. For deciduous needleleaf forest and tundra, both $\beta_{p_{sun}}$ ($\beta_{p_{sha}}$) and $\beta_{S_{sun}}$ ($\beta_{S_{sha}}$) contribute to the maginitudes and trends of $\beta_{GPP_{sun}}(\beta_{GPP_{sha}})$. For evergreen needleleaf forest, deciduous broadleaf forest, shrub and $C_3$ grass, $\beta_{S_{sun}}$ ($\beta_{S_{sha}}$) dominates the magnitude and change of $\beta_{GPP_{sun}}(\beta_{GPP_{sha}})$. For evergreen broadleaf forest, $\beta_{S_{sha}}$ predominates before 2035.

## 4. Discussion

### 4.1 Variation of biochemical and leaf-level photosynthetic responses to eCO₂

Most previous studies focused on variation in $\beta$ for the land carbon storage, the standard definition of $\beta$ as in Friedlingstein et al. (2006). However, accurate estimate of leaf-level $\beta$ has not been attempted by modelling groups before. In this study, with the available outputs of biochemical parameters $C_i$ and $\Gamma_*$ in CABLE model, we calculated leaf-level $\beta$ values with distinction of sunlit and shaded leaves for the first time. The calculation of leaf-level $\beta$ simply through the sensitivity of GPP/LAI might lead to biases because some models used two-leaf or multiple-layer canopy structure. In our study, we also compared the sensitivities of GPP/LAI with leaf-level $\beta$ values derived from $C_i$ and $\Gamma_*$. Results show that the former calculation causes large biases, especially for trees (Fig.S5). Thus, the relatively large divergence of the sensitivities of GPP/LAI to eCO₂ in Hajima et al. (2014) may not indicate diverse leaf-level photosynthesis responses among CMIP5 models. Another advantage of our calculation of leaf-level $\beta$ is that the reason for the divergence of leaf-level $\beta$ within and across vegetation types can be traced back to difference from $C_i$ and leaf temperature as shown in Fig.2.

The direct CO₂ fertilization effect occurs at leaf level and is determined by kinetic sensitivity of Rubisco enzymes to internal leaf CO₂. In fact, the normalized short-term sensitivity of leaf level photosynthesis to CO₂ is mainly regulated by intercellular CO₂ concentration $C_i$ and slightly influenced by leaf temperature, regardless of light, nutrient availability, and species characteristics (Luo et al., 1996; Luo & Mooney, 1996). In our study, modelled $C_i/C_a$ values are approximately constant with eCO₂ for a specific vegetation type, and vary little within and across vegetation types. This is in line with FACE experimental results which show almost constant $C_i/C_a$ values for different vegetation types under eCO₂ conditions (Drake et al., 1997; Long et al., 2004). Previous research showed that global temperature variation only caused a small influence on biochemical response $\mathcal{L}$ (Luo & Mooney, 1996). Therefore, biochemical and leaf-level $\beta$ vary little within and among global vegetation types in this study.

In this study, we assume values of $j_{cmax,25}$ and $v_{cmax,25}$ are PFT-specific and do not change with time. In fact, downregulation of photosynthesis is observed in experiments when plants acclimate to eCO₂ in the long term. Downregulation

310    involves reduction in $v_{cmax,25}$ by about 13% and $j_{cmax,25}$ by about 5% on average (Long et al., 2004). Then the leaf

biochemical response $\mathcal{L}'$ for Rubisco-limit and RuBP-limit should be written as:

$$\mathcal{L}'_1 = \mathcal{L}_1 + \frac{1}{v_{cmax,25}} * \frac{dv_{cmax,25}}{dCi} \tag{29}$$

$$\mathcal{L}'_2 = \mathcal{L}_2 + \frac{1}{j_{cmax,25}} * \frac{dj_{cmax,25}}{dCi} \tag{30}$$

Where $\mathcal{L}_1$ and $\mathcal{L}_2$ are the leaf biochemical responses without the influence from shifts in $v_{cmax,25}$ and $j_{cmax,25}$. $\mathcal{L}'$ will

315    become smaller because of the reduction of $v_{cmax,25}$ and $j_{cmax,25}$. And it has been observed that $j_{cmax,25}$ and $v_{cmax,25}$

tended to be reduced to a greater extent in grasses and shrubs than in trees (Ainsworth & Long, 2005). Due to the

downregulation mechanism, the leaf biochemical response to $eCO_2$ will diverge more among different $C_3$ functional groups.

**4.2 Variation of $\beta$ at canopy and ecosystem levels**

The two-leaf scaling scheme in CABLE is widely employed by many land surface models, such as Community Land Model

320    version 4.5 (CLM4.5, Bonan et al., 2013) and the Joint UK Land Environment Simulator version 4.5 (JULES4.5, Best et al.,

2011; Clark et al., 2011; Harper et al., 2016). We found the responses of ecosystem carbon cycle to $eCO_2$ diverge primarily

because the responses of LAI diverge within and among vegetation types. Besides, GPP of shaded leaves responds stronger

than that of sunlit leaves for all $C_3$ plants. This is because the LAI-dependent scaling factor of shaded leaves increase

exponentially with increasing LAI, leading to a rapid change of GPP. Our results also indicate that saturation of GPP is not

325    only regulated by the leaf-level response, but also by the response of the scaling factors to $eCO_2$. For shaded leaves, the

sensitivity of the scaling factor contributes more to the magnitude and trend of $\beta_{GPP_{sha}}$. The evidence all suggests LAI is a

key process in modeling the response of ecosystem carbon cycle to climate change.

It has been reported that LAI is overestimated in CMIP5 historical simulations compared with remote sensing LAI products

330    (Anav et al., 2013). Also, many global vegetation models predict increasing LAI in response to $eCO_2$. Our study also show

that LAI responds positively to $eCO_2$ for all $C_3$ plants. But experimental results are not consistent. In one review paper with

12 FACE experimental results, trees had a 21% increase in LAI, herbaceous $C_3$ grasses did not show a significant change in

LAI (Ainsworth & Long, 2005). While some studies reported that LAI dynamics did not significantly change in specific FACE

experiments, such as in a high-LAI deciduous broadleaf forest (Norby et al., 2003) and in a low-LAI evergreen broadleaf forest

335    (Duursma et al., 2016). In this study, modelled $\beta$ effects at the canopy-level are higher than those at the leaf-level for all $C_3$

plants, whereas it is generally observed in experiments that the leaf-level response is consistently larger than the whole plant

response (Long et al., 2006; Leuzinger et al., 2011). One possible reason is that models overestimate the response of LAI to

$eCO_2$, as this study has shown that LAI is an important factor in driving ecosystem response to $CO_2$ fertilization. And it is also

likely the overestimation of the response of LAI to $eCO_2$ is responsible for the overestimation of $CO_2$ fertilization in ESMs

340    reported by previous studies (Smith et al., 2015; Mystakidis et al., 2017).

In CABLE, the variation of the response of LAI to $eCO_2$ within a certain vegetation type is mainly dominated by environmental

factors such as temperature, radiation and water. While for different vegetation types, diverse seasonal dynamics of leaf growth

introduce additional variation. The overall response of LAI to $eCO_2$ depends on several processes in this study: (1) NPP

345    increment, (2) change in allocation of NPP to leaf, (3) change in specific leaf area (SLA) in response to $eCO_2$, (4) PFT-specific

minimum and maximum LAI values prescribed in the model. Insensitive responses of LAI to $eCO_2$ for deciduous needleleaf

forest and tundra can be attributed to smaller NPP enhancements in cold areas. Accurate estimate of GPP and NPP is therefore

fundamental to realistic LAI modeling. Second, we assume that allocation fractions are not affected by environmental

conditions by fixing allocation coefficients in this study. However, results from two FACE (Duke Forest and Oak Ridge)

350    experiments indicate that the carbon allocated to leaves is decreased and more carbon is allocated to woods or roots at higher

$CO_2$ concentration (De Kauwe et al., 2014). Third, we fixed SLA to calculate LAI in CABLE. But a reduction in SLA is a

commonly observed response in $eCO_2$ experiments (Ainsworth et al., 2005; De Kauwe et al., 2014). Tachiiri et al. (2012) also

found SLA and $\beta$ values are most effectively constrained by observed LAI to smaller values in a model. Therefore, the fixed

SLA may also lead to over-prediction of the response of canopy cover to $eCO_2$. Finally, in our results, LAI values for most $C_3$

355    plants are below the maximum LAI limits with $eCO_2$. With only one exception, LAI values of many evergreen broadleaf forest

Biogeosciences
Discussions

patches saturate at the prescribed maximum value in response to eCO$_2$ (Fig. S6 and Table. S1). That's why the sensitivity of

LAI for evergreen broadleaf forest is low and thus leads to small relative GPP and NPP enhancements. If the preset LAI upper

limits are narrowed, $\beta$ effects might be significantly reduced. Hence model parameters related to LAI need to be better

calibrated according to experiments and observations in order to better represent the response of ecosystem productivity to

360   eCO$_2$ (Qu & Zhuang, 2018).

In this study, the almost identical values and variance of $\beta_{NPP}$ as those of $\beta_{GPP}$ within and across C$_3$ plants suggests carbon

use efficiency does not change with eCO$_2$, as autotrophic respiration is calculated from GPP and plant carbon. The reduced

magnitudes of $\beta_{cpool}$ compared with those of $\beta_{GPP}$ and $\beta_{NPP}$ indicates carbon turnover processes make ecosystems

365   respond to eCO$_2$ less sensitively. A previous study using seven global vegetation models identified carbon residence time as

the dominant uncertainty in terrestrial vegetation responses to future climate and atmospheric CO$_2$ change (Friend et al., 2014).

The response of soil carbon storage to eCO$_2$ also depends on carbon turnover time (Harrison et al., 1993). In our study, soil

decomposition rate is assumed not to be affected by CO$_2$ level, as in most other conventional soil carbon models (Friedlingstein

et al., 2006; Luo et al., 2016). However, recent synthesis of experimental data suggests eCO$_2$ increases turnover rate of new

370   soil carbon (Van Groenigen et al., 2014; Van Groenigen et al., 2016). Within a certain vegetation type, the variation of $\beta_{cpool}$

across different geographical locations is usually not as large as that of $\beta_{NPP}$. But the greatest variation of $\beta_{cpool}$ among

different C$_3$ plants compared with variations of $\beta_{GPP}$ and $\beta_{NPP}$ suggests other processes such as different carbon allocation

patterns, plant carbon turnover, and the soil carbon dynamics of various vegetation types, are responsible for the divergence.

375   It should be noted that our study was designed to identify the key process that influences CO$_2$ fertilization effects without

considering nitrogen and phosphorus interactions. $\beta$ effects might be over-estimated by the neglect of nutrient limitations on

plant growth (Hungate et al., 2003; Luo et al., 2004; Thornton et al., 2009). Uncertainty still exists in the response of ecosystem

carbon dynamics to eCO$_2$ with nutrient interactions. Current terrestrial carbon-nitrogen cycle models cannot capture the

response of NPP to eCO$_2$ in FACE experiments. They also disagree with each other on the responses of nitrogen-based GPP

380    and NPP to eCO$_2$ because they have diverse mechanisms of C-N coupling (Zaehle et al., 2014).

### 4.3 Implication for understanding the uncertainty of $\beta$ values among models

Our theoretical analysis of variability of $\beta$ values at different levels within and across several plant functional types in

CABLE model can offer insights into inter-modal variation of $\beta$ values revealed by model intercomparison projects. The

basic photosynthesis model and two-leaf scaling scheme in CABLE model are shared by many land surface models. It can be

385    inferred that normalized leaf-level $\beta$ values would diverge little across different land surface models as long as they use

Farquhar photosynthesis model with similar expressions for intercellular CO$_2$ concentration ($C_i$) , Michaelis-Menten constants

($K_c$, $K_o$) and CO$_2$ compensation point in the absence of day respiration ($\Gamma_*$) (Luo et al., 1996; Luo & Mooney, 1996). A recent

study used 16 crop models to predict rice yield in response to eCO$_2$ (Hasegawa et al., 2017). They found the variation of yield

response across models was not associated with model structure or magnitude of primary photosynthetic response to eCO$_2$,

390    but was significantly related with the predictions of leaf area. This is consistent with our conclusion about the relative

conservative character of leaf-level $\beta$. The high association between the response of LAI and response of yield among those

models extends our conclusion about internal association between these two variables within a model, highlighting the great

need to improve prognostic LAI modeling.

395    Although we analyze a single land-surface model in detail, we suspect our top-level conclusions will be generally applicable.

We therefore invite other land-surface modelling groups to similarly analyze their model estimates of $\beta$ at different

hierarchical levels across different geographical locations and vegetation types as we did, and focus more on contributions

from change in leaf-level photosynthesis, changes in leaf area index and changes in land carbon residence times.

Biogeosciences

Discussions

Open Access

EGU

## 5. Conclusions

400   Exploring the variability of $\beta$ effects at different hierarchical levels within and across different plant types helps reveal model

mechanisms that govern terrestrial ecosystem responses to elevated $CO_2$. Our study using the CABLE model shows that the

sensitivities of biochemical and leaf-level photosynthesis to $eCO_2$ are very similar within and among $C_3$ plants, in accordance

with previous theoretical analysis. While $\beta$ values of GPP, NPP and ecosystem carbon storage diverge primarily because the

sensitivities of LAI to $eCO_2$ significantly differ within and across vegetation types. After decomposing $\beta$ values of sunlit and

405   shaded leaf GPP into $\beta$ of leaf-level photosynthesis and the LAI-dependent leaf-to-canopy scaling factor, we find the latter

to be the most important cause of the divergence of model responses. Our results indicate that processes related to LAI need

to be better constrained with experiments and observations in order to better represent the response of ecosystem carbon cycle

to $eCO_2$.

## References

415

Ainsworth, E. A., & Long, S. P. 2005. What have we learned from 15 years of free-air $CO_2$ enrichment (FACE)? A meta-
analytic review of the responses of photosynthesis, canopy properties and plant production to rising $CO_2$. *New Phytologist*,
**165** 351-372.

Anav, A., Friedlingstein, P., Kidston, M., Bopp, L., Ciais, P., Cox, P., ... & Zhu, Z. 2013. Evaluating the land and ocean

420      components of the global carbon cycle in the CMIP5 Earth System Models. *Journal of Climate*, **26** 6801-43.

Arora VK, Boer GJ, Eby M et al. 2013. Carbon–Concentration and Carbon–Climate Feedbacks in CMIP5 Earth System
Models. *dx.doi.org*, **26** 5289–314.

Best, M. J., Pryor, M., Clark, D. B., Rooney, G. G., Essery, R., Ménard, C. B., ... & Mercado, L. M. 2011. The Joint UK Land Environment Simulator (JULES), model description–Part 1: energy and water fluxes. *Geoscientific Model Development*, **4** 677-99.

Bonan GB, Levis S 2010. Quantifying carbon-nitrogen feedbacks in the Community Land Model (CLM4). *Geophysical Research Letters*, **37**.

Bonan, G. B., Drewniak, B., & Huang, M. 2013. *Technical Description of Version 4.5 of the Community Land Model (CLM)* (NCAR Technical Note NCAR/TN-503+ STR, Boulder, Colorado) pp. 259-74.

Canadell, J. G., Pataki, D. E., Gifford, R., Houghton, R. A., Luo, Y., Raupach, M. R., ... & Steffen, W. 2007. Saturation of the terrestrial carbon sink (pp. 59-78). *Springer Berlin Heidelberg*.

Clark, D. B., Mercado, L. M., Sitch, S., Jones, C. D., Gedney, N., Best, M. J., ... & Boucher, O. 2011. The Joint UK Land Environment Simulator (JULES), model description-Part 2: carbon fluxes and vegetation dynamics. *Geoscientific Model Development*, **4** 701.

Collatz, G. J., Ball, J. T., Grivet, C., & Berry, J. A. 1991. Physiological and environmental regulation of stomatal conductance, photosynthesis and transpiration: a model that includes a laminar boundary layer. *Agricultural and Forest Meteorology*, **54** 107-36.

Collatz, G. J., Ribas-Carbo, M., & Berry, J. A. 1992. Coupled photosynthesis-stomatal conductance model for leaves of C4 plants. *Functional Plant Biology*, **19** 519-38.

Cox P. M., Betts RA, Jones CD, Spall SA, Totterdell IJ. 2000. Acceleration of global warming due to carbon-cycle feedbacks in a coupled climate model. *Nature*, **408** 184–7.

Cox, P. M. 2001. Description of the TRIFFID dynamic global vegetation model. *Hadley Centre technical note*, **24** 1-16.

De Kauwe, M. G., Medlyn, B. E., Zaehle, S., Walker, A. P., Dietze, M. C., Wang, Y. P., ... & Wårlind, D. 2014. Where does the carbon go? A model–data intercomparison of vegetation carbon allocation and turnover processes at two temperate forest free-air $CO_2$ enrichment sites. *New Phytologist*, **203** 883-99.

Duursma, R. A., Gimeno, T. E., Boer, M. M., Crous, K. Y., Tjoelker, M. G., & Ellsworth, D. S. 2016. Canopy leaf area of a mature evergreen Eucalyptus woodland does not respond to elevated atmospheric [CO2] but tracks water availability. *Global change biology*, **22** 1666-1676.

Drake, B. G., Gonzàlez-Meler, M. A., & Long, S. P. 1997. More efficient plants: a consequence of rising atmospheric $CO_2$? *Annual review of plant biology*, **48** 609-39.

Ewert, F. 2004. Modelling plant responses to elevated $CO_2$: how important is leaf area index? *Annals of botany*, **93** 619-627.

Fatichi, S., Leuzinger, S., Paschalis, A., Langley, J. A., Barraclough, A. D., & Hovenden, M. J. 2016. Partitioning direct and indirect effects reveals the response of water-limited ecosystems to elevated $CO_2$. *Proceedings of the National Academy of Sciences*, **113** 12757-62.

455  Farquhar, G. V., von Caemmerer, S. V., & Berry, J. A. 1980. A biochemical model of photosynthetic $CO_2$ assimilation in leaves of C3 species. *Planta*, **149** 78-90.

Friedlingstein P, Cox P, Betts R et al. 2006. Climate–Carbon Cycle Feedback Analysis: Results from the C4MIP Model Intercomparison. *Journal of Climate*, **19** 3337–53.

Friedlingstein P. 2015. Carbon cycle feedbacks and future climate change. *Phil. Trans. R. Soc. A*, **373** 20140421.

460  Friend, A. D., Lucht, W., Rademacher, T. T., Keribin, R., Betts, R., Cadule, P., ... & Ito, A. 2014. Carbon residence time dominates uncertainty in terrestrial vegetation responses to future climate and atmospheric $CO_2$. *Proceedings of the National Academy of Sciences*, **111** 3280-5.

Fung, I. Y., Doney, S. C., Lindsay, K., & John, J. 2005. Evolution of carbon sinks in a changing climate. *Proceedings of the National Academy of Sciences of the United States of America*, **102** 11201-6.

465  Gregory, J. M., Jones, C. D., Cadule, P., & Friedlingstein, P. 2009. Quantifying carbon cycle feedbacks. *Journal of Climate*, **22** 5232-50.

Hajima, T., Tachiiri, K., Ito, A., & Kawamiya, M. 2014. Uncertainty of Concentration–Terrestrial Carbon Feedback in Earth System Models*. *Journal of Climate*, **27** 3425-45.

Harper, A. B., Cox, P. M., Wiltshire, A. J., Jones, C. D., Mercado, L. M., Atkin, O. K., ... & Soudzilovskaia, N. A. 2016.
470  Improved representation of plant functional types and physiology in the Joint UK Land Environment Simulator (JULES v4. 2) using plant trait information. *Geoscientific Model Development*, **9** 2415.

Harrison, K., Broecker, W., & Bonani, G. 1993. A strategy for estimating the impact of $CO_2$ fertilization on soil C storage. *Global Biochemical Cycles*, **7** 69-80.

Hasegawa, T., Li, T., Yin, X., Zhu, Y., Boote, K., Baker, J., ... & Fumoto, T. 2017. Causes of variation among rice models in
475  yield response to CO 2 examined with Free-Air CO 2 Enrichment and growth chamber experiments. *Scientific Reports*, **7** 14858.

Heimann, M., & Reichstein, M. 2008. Terrestrial ecosystem carbon dynamics and climate feedbacks. *Nature*, **451** 289.

Hungate, B. A., Dukes, J. S., Shaw, M. R., Luo, Y., & Field, C. B. 2003. Nitrogen and climate change. *Science*, **302** 1512-3.

Iversen, C. M., Keller, J. K., Garten, C. T., & Norby, R. J. 2012. Soil carbon and nitrogen cycling and storage throughout the
480  soil profile in a sweetgum plantation after 11 years of $CO_2$-enrichment. *Global Change Biology*, **18** 1684-97.

Joos, F., Prentice, I. C., Sitch, S., Meyer, R., Hooss, G., Plattner, G. K., ... & Hasselmann, K. 2001. Global warming feedbacks on terrestrial carbon uptake under the Intergovernmental Panel on Climate Change (IPCC) emission scenarios. *Global Biogeochemical Cycles*, **15** 891-907.

Le Quéré, C., Moriarty, R., Andrew, R. M., Canadell, J. G., Sitch, S., Korsbakken, J. I., ... & Houghton, R. A. 2015. Global
485  carbon budget 2015. *Earth System Science Data*, **7** 349-96.

Leuning, R. 1990. Modelling stomatal behaviour and and photosynthesis of *Eucalyptus grandis*. *Functional Plant Biology*, **17** 159-75.

Leuzinger, S., Luo, Y., Beier, C., Dieleman, W., Vicca, S., & Körner, C. 2011. Do global change experiments overestimate impacts on terrestrial ecosystems? *Trends in ecology & evolution*, **26** 236-41.

490 Long, S. P., Ainsworth, E. A., Rogers, A., & Ort, D. R. 2004. Rising atmospheric carbon dioxide: plants FACE the Future*. *Annu. Rev. Plant Biol.,* **55** 591-628.

Long, S. P., Ainsworth, E. A., Leakey, A. D., Nösberger, J., & Ort, D. R. 2006. Food for thought: lower-than-expected crop yield stimulation with rising $CO_2$ concentrations. *Science*, **312** 1918-1921.

Luo, Y., Sims, D. A., Thomas, R. B., Tissue, D. T., & Ball, J. T. 1996. Sensitivity of leaf photosynthesis to $CO_2$ concentration
495 is an invariant function for C3 plants: A test with experimental data and global applications. *Global Biochemical Cycles*, **10** 209-222.

Luo, Y. and H.A. Mooney. 1996. Stimulation of global photosynthetic carbon influx by an increase in atmospheric carbon dioxide concentration. (In G.W. Koch and H.A. Mooney (eds.) *Carbon Dioxide and Terrestrial Ecosystems.* Academic Press, San Diego) pp. 381-97.

500 Luo, Y., Su, B. O., Currie, W. S., Dukes, J. S., Finzi, A., Hartwig, U., ... & Pataki, D. E. 2004. Progressive nitrogen limitation of ecosystem responses to rising atmospheric carbon dioxide. *AIBS Bulletin*, **54** 731-9.

Luo, Y., Ahlström, A., Allison, S. D., Batjes, N. H., Brovkin, V., Carvalhais, N., ... & Georgiou, K. 2016. Toward more realistic projections of soil carbon dynamics by Earth system models. *Global Biochemical Cycles*, **30** 40-56.

Matthews, H. D., Eby, M., Weaver, A. J., & Hawkins, B. J. 2005. Primary productivity control of simulated carbon cycle–
505 climate feedbacks. *Geophysical research letters*, **32**.

Mystakidis, S., Seneviratne, S. I., Gruber, N., & Davin, E. L. 2017. Hydrological and biogeochemical constraints on terrestrial carbon cycle feedbacks. *Environmental Research Letters*, **12** 014009.

Norby, R. J., Sholtis, J. D., Gunderson, C. A., & Jawdy, S. S. 2003. Leaf dynamics of a deciduous forest canopy: no response to elevated $CO_2$. Oecologia, **136** 574-584.

510 Peng, J., Dan, L., & Huang, M. 2014. Sensitivity of global and regional terrestrial carbon storage to the direct CO2 effect and climate change based on the CMIP5 model intercomparison. *PloS one*, **9** e95282.

Qu, Y., & Zhuang, Q. 2018. Modeling leaf area index in North America using a process‐based terrestrial ecosystem model. *Ecosphere*, **9**.

Smith, W. K., Reed, S. C., Cleveland, C. C., Ballantyne, A. P., Anderegg, W. R., Wieder, W. R., ... & Running, S. W. 2016.
515 Large divergence of satellite and Earth system model estimates of global terrestrial $CO_2$ fertilization. *Nature Climate Change*, **6** 306-10.

Tachiiri, K., Akihiko, I. T. O., Hajima, T., Hargreaves, J. C., Annan, J. D., & Kawamiya, M. 2012. Nonlinearity of land carbon sensitivities in climate change simulations. *Journal of the Meteorological Society of Japan. Ser. II*, **90** 259-74.

Thornton, P. E., Doney, S. C., Lindsay, K., Moore, J. K., Mahowald, N., Randerson, J. T., ... & Lee, Y. H. 2009. Carbon-
520 nitrogen interactions regulate climate-carbon cycle feedbacks: results from an atmosphere-ocean general circulation model. *Biogeosciences*, **6**.

Van Groenigen, K. J., Qi, X., Osenberg, C. W., Luo, Y., & Hungate, B. A. 2014. Faster decomposition under increased atmospheric $CO_2$ limits soil C storage. *Science*, 1249534.

van Groenigen, K. J., Osenberg, C. W., Terrer, C., Carrillo, Y., Dijkstra, F., Heath, J., ... & Hungate, B. A. 2016. Faster turnover
525         of new soil carbon inputs under increased atmospheric $CO_2$. *Global Change Biology*.

Wang, Y. P., & Leuning, R. 1998. A two-leaf model for canopy conductance, photosynthesis and partitioning of available energy I:: Model description and comparison with a multi-layered model. *Agricultural and Forest Meteorology*, **91** 89-111.

Wang, Y. P., Law, R. M., & Pak, B. 2010. A global model of carbon, nitrogen and phosphorus cycles for the terrestrial
530         biosphere. *Biogeosciences,* **7** 2261.

Wang, Y. P., Kowalczyk, E., Leuning, R., Abramowitz, G., Raupach, M. R., Pak, B., ... & Luhar, A. 2011. Diagnosing errors in a land surface model (CABLE) in the time and frequency domains. *Journal of Geophysical Research: Biogeosciences*, **116**.

Zaehle, S., Medlyn, B. E., De Kauwe, M. G., Walker, A. P., Dietze, M. C., Hickler, T., ... & Jain, A. 2014. Evaluation of 11
535         terrestrial carbon–nitrogen cycle models against observations from two temperate Free-Air $CO_2$ Enrichment studies.
        *New Phytologist*, **202** 803-22.

Zeng N. 2004. How strong is carbon cycle-climate feedback under global warming? *Geophysical Research Letters*, **31** L20203–5.

**Table 1 Coefficients of variation of $\mathcal{L}$, $dC_i/dC_a$, $\beta_p$, $\beta_{LAI}$, $\beta_{GPP}$, $\beta_{NPP}$ and $\beta_{cpool}$ across different geographical locations within each C₃ vegetation type. The two numbers in the same unit are for sunlit leaves and shaded leaves respectively. Values for shaded leaves are in brackets. Abbreviations are the same as Figure 1.**

|  | ENF | EBF | DNF | DBF | SHB | C3GRAS | TUN |
|---|---|---|---|---|---|---|---|
| CV($\mathcal{L}$) | 0.25(0.30) | 0.27(0.29) | 0.25(0.27) | 0.39(0.39) | 0.33(0.33) | 0.39(0.35) | 0.34(0.33) |
| CV($dC_i/dC_a$) | 0.21(0.16) | 0.09(0.07) | 0.1(0.09) | 0.14(0.11) | 0.08(0.28) | 0.10(0.08) | 0.1(0.09) |
| CV($\beta_p$) | 0.47(0.36) | 0.25(0.29) | 0.27(0.26) | 0.44(0.37) | 0.33(0.41) | 0.40(0.36) | 0.34(0.33) |
| CV($\beta_{LAI}$) | 3.21 | 1.43 | 1.15 | 1.49 | 1.56 | 2.18 | 3.83 |
| CV($\beta_{GPP}$) | 2.73 | 0.43 | 0.95 | 1.22 | 1.27 | 1.14 | 1.75 |
| CV($\beta_{NPP}$) | 4.78 | 0.38 | 0.96 | 1.41 | 1.30 | 1.11 | 1.73 |
| CV($\beta_{cpool}$) | 1.28 | 0.46 | 0.37 | 0.80 | 0.98 | 0.99 | 1.85 |
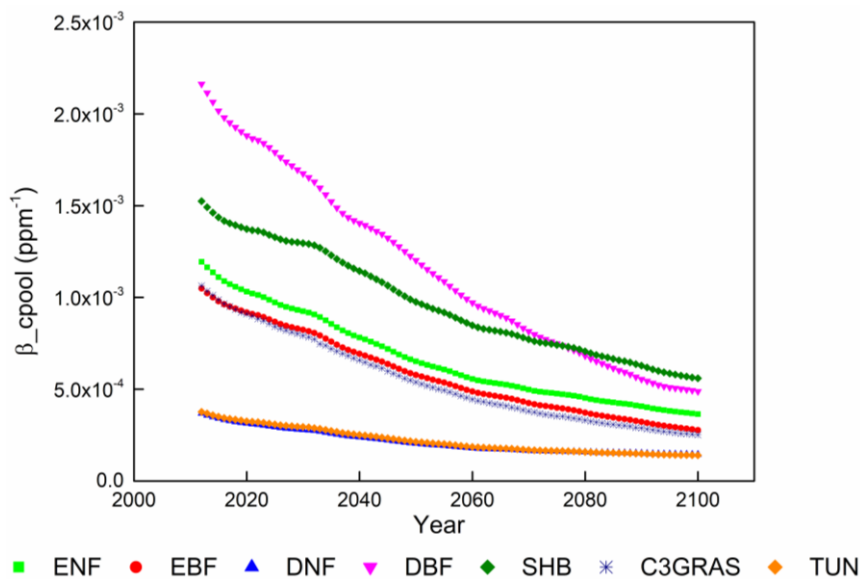
**Figure 1 Temporal trends of $\beta_{cpool}$ from 2011 to 2100 for C$_3$ plants in CABLE. $\beta_{cpool}$ values for different C$_3$ plants**

545 **all decline with time from 2011 to 2100 under RCP8.5 scenario, but the magnitudes of $\beta_{cpool}$ differ across them. ENF, Evergreen Needle leaf Forest (light green square); EBF, Evergreen Broad leaf Forest (red circle); DNF, Deciduous Needle leaf Forest (dark blue triangle); DBF, Deciduous Broad leaf Forest (pink triangle); SHB, Shrub (dark green diamond); C3GRAS, C$_3$ grass (dark blue star); TUN, tundra (orange diamond).**
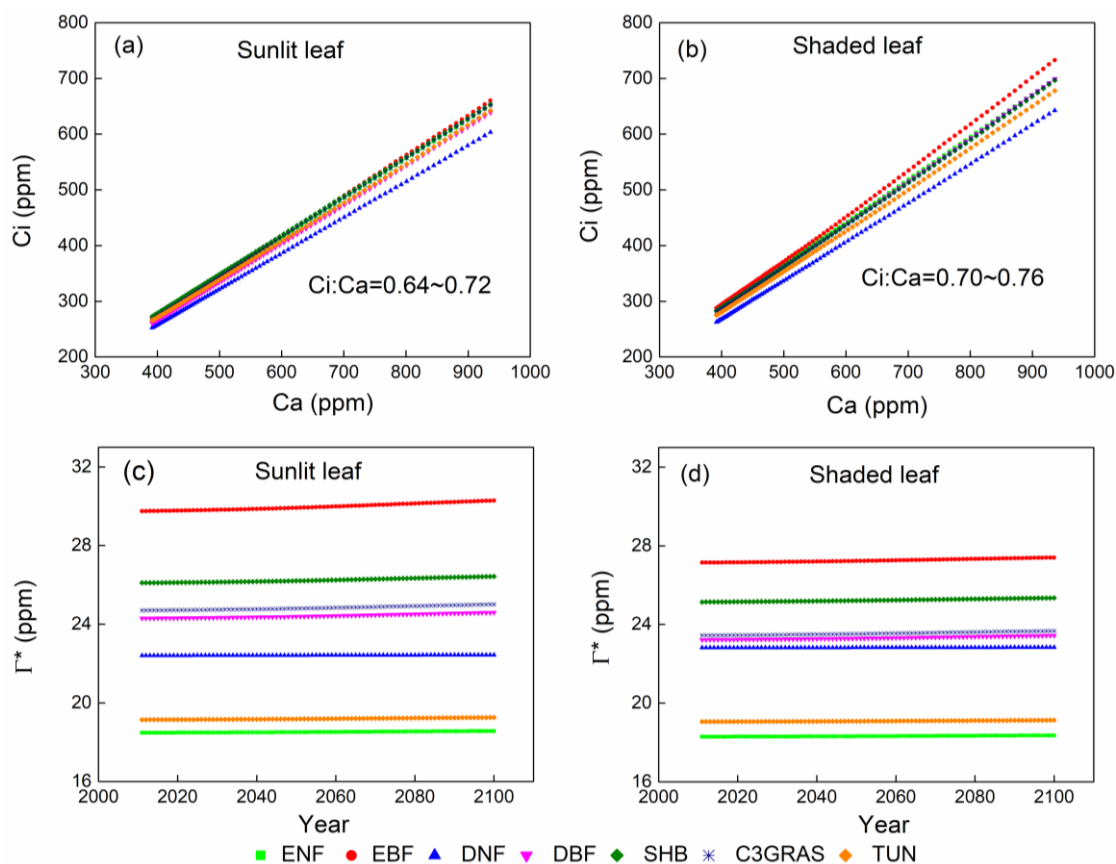
550

**Figure 2 Responses of yearly intercellular CO₂ concentration to eCO₂ of a single sunlit leaf (a) and shaded leaf (b) for C₃ plants. Temporal trends of CO₂ compensation point in the absence of day respiration ($\Gamma_*$) for sunlit leaf (c) and shaded leaf (d) from 2011 to 2100 in CABLE. The ratios of $C_i$ to $C_a$ ($C_i/C_a$) are approximately constants with eCO₂ for each vegetation type and vary little between vegetation types. $\Gamma_*$ values vary across global vegetation types, but do not change through time for each vegetation type. Abbreviations and symbols are the same as Figure 1.**

555
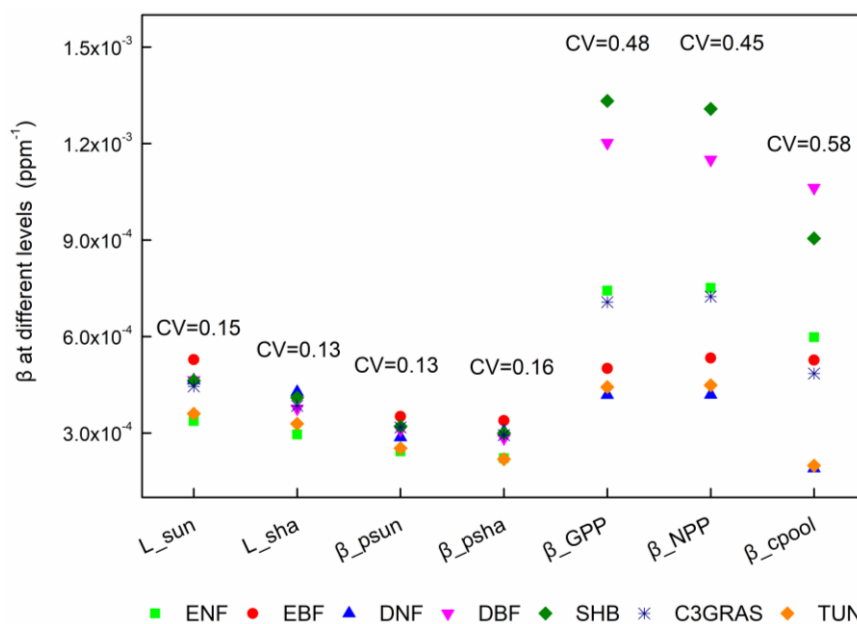
**Figure 3** $\beta$ values at different levels for various C$_3$ plants at the year 2056 in CABLE. CV means coefficient of variation among C$_3$ plants. $\beta$ values at biochemical and leaf-level are very similar among vegetation types, but greatly diverge at GPP, NPP and ecosystem carbon storage level. Abbreviations and symbols are the same as Figure 1.

560

565

570
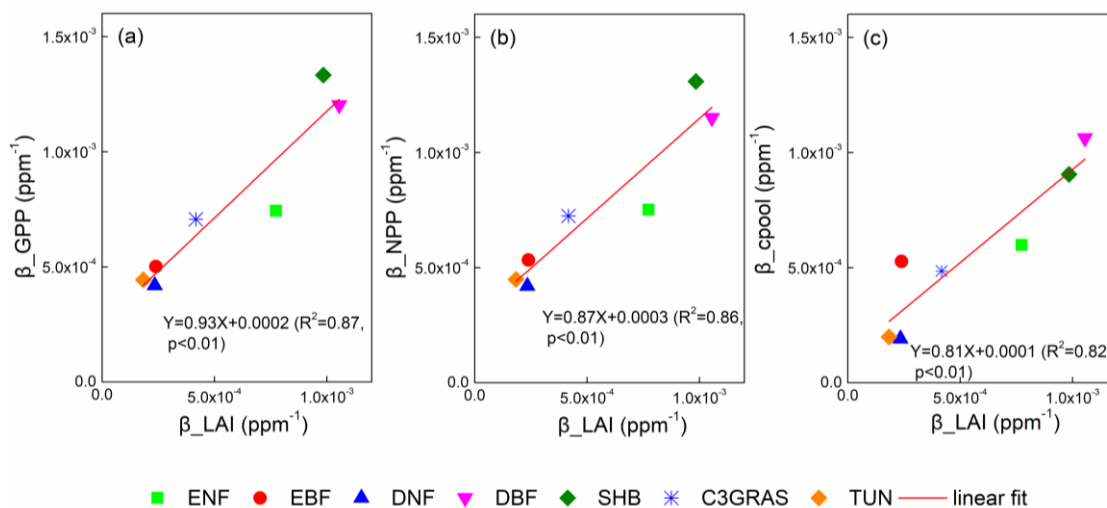
**Figure 4 Correlations between $\beta_{\text{GPP}}$ and $\beta_{\text{LAI}}$ (a), $\beta_{\text{NPP}}$ and $\beta_{\text{LAI}}$ (b), $\beta_{\text{cpool}}$ and $\beta_{\text{LAI}}$ (c) at the year 2056 among C3 plants in CABLE. $\beta_{\text{GPP}}$, $\beta_{\text{NPP}}$ and $\beta_{\text{cpool}}$ all have significant linear correlations with $\beta_{\text{LAI}}$ but with different slopes. Abbreviations and symbols are the same as Figure 1.**

575

580

585
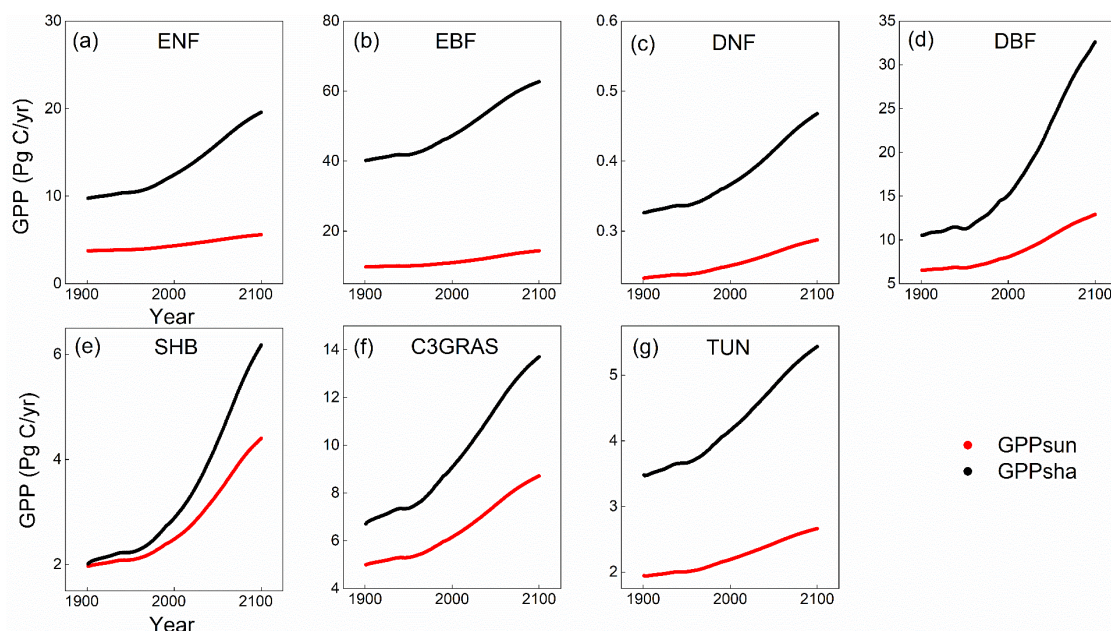
**Figure 5 Temporal trends of GPP$_{sun}$ (red point) and GPP$_{sha}$ (black point) for C$_3$ plants from 1901 to 2100 in CABLE. GPP$_{sha}$ is higher than GPP$_{sun}$ for almost all vegetation types. With significant increase of CO$_2$ concentration from 590 2011, GPP$_{sha}$ responds more drastically than GPP$_{sun}$.**

595

Biogeosciences
Discussions

Open Access

EGU
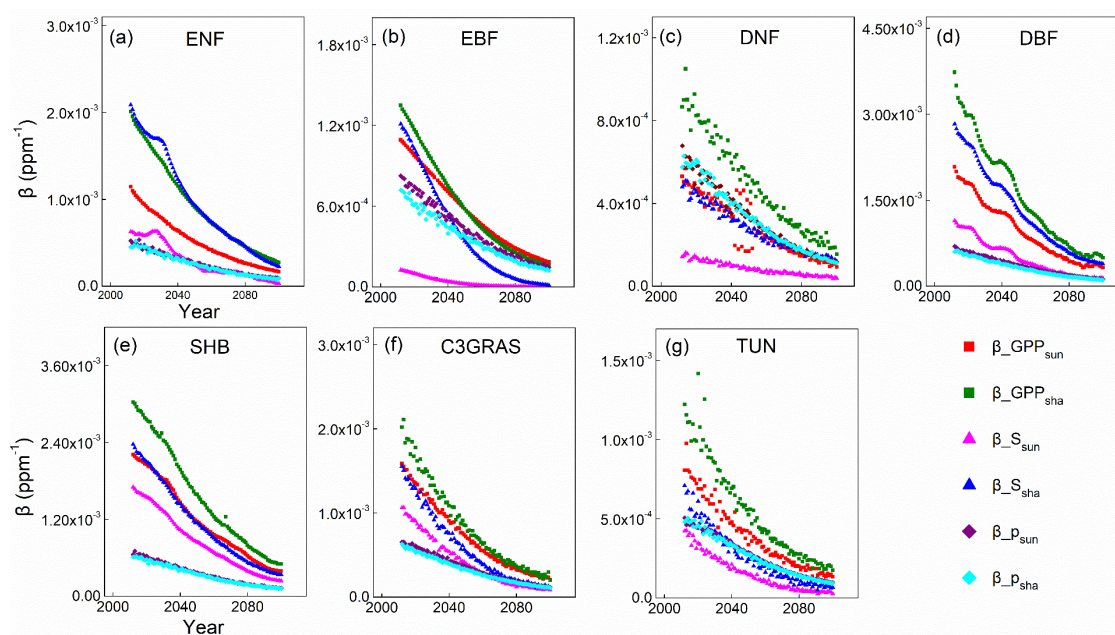


**Figure 6 Temporal trends of** $\beta_{\mathrm{GPP}_{sun}}$ **(red square),** $\beta_{\mathrm{GPP}_{sha}}$ **(green square),** $\beta_{S_{sun}}$ **(pink triangle),** $\beta_{S_{sha}}$ **(dark blue triangle),** $\beta_{p_{sun}}$ **(purple diamond) and** $\beta_{p_{sha}}$ **(sky blue diamond) for C₃ plants in CABLE. The sensitivities of** $\mathrm{GPP}_{sun}$ **and** $\mathrm{GPP}_{sha}$ **tend to approach zero through time because the decomposing factors** $\beta_{p_{sun}}$, $\beta_{p_{sha}}$, $\beta_{S_{sun}}$ **and** $\beta_{S_{sha}}$ **all decline with time.** $\beta_{S_{sha}}$ **determines the magnitudes and trends of** $\beta_{\mathrm{GPP}_{sha}}$ **for almost all vegetation types.**